第 33 卷第 6 期
2017 年 6 月

无 机 化 学 学 报
CHINESE JOURNAL OF INORGANIC CHEMISTRY

Vol.33 No.6
913-922

氧杂蒽染料修饰钴–硫脲配合物的光解水放氢性能

杨林林 景 旭 何 成* 段春迎
(大连理工大学精细化工重点实验室,大连 116024)

摘要:将具有不同端基的硫脲基团与三苯基磷组分结合,利用所得到的配体合成了 2 个具有 NSP(氮硫磷)螯合位点的钴–硫脲化合物,并研究了其光解水产氢性能。配合物[Co(L2)(L2′)]$(BF_4)_{2.5}\cdot H_2O\cdot 0.5C_2H_5OH$ (**2**)(L2=(2-二苯基膦–苯烯基)–氨基硫脲腙–罗丹明 6G,L2′=(2-二苯基膦氧–苯烯基)–氨基硫脲腙–罗丹明 6G)通过引入罗丹明荧光团与光敏剂分子协同作用,其产氢 TON 值可以达到 2 800 $mol_{H_2}\cdot mol_{cat}^{-1}$,其初始 TOF 值可达到 930 $mol_{H_2}\cdot mol_{cat}^{-1}\cdot h^{-1}$。相同条件下,相比于配合物[Co(L1)(L1′)]$(BF_4)\cdot 0.5H_2O$ (**1**)(L1=(2-二苯基膦–苯烯基)–氨基硫脲腙–硫甲基,L1′=(2-二苯基膦氧–苯烯基)–氨基硫脲腙–硫甲基),提高了体系的催化活性,可能是由于荧光素分子与配合物 **2** 之间的分子间 π-π 堆积作用有利于光敏剂和光催化剂之间的光致电子转移。

关键词:光致电子转移;钴;硫脲;光催化产氢
中图分类号:O614.81+2 **文献标识码**:A **文章编号**:1001-4861(2017)06-0913-10
DOI:10.11862/CJIC.2017.126

Photocatalytic Hydrogen Production Based on Cobalt-Thiosemicarbazone Complex with the Xanthene Dye Moiety

YANG Lin-Lin JING Xu HE Cheng* DUAN Chun-Ying
(*State Key Laboratory of Fine Chemicals, Dalian University of Technology, Dalian, Liaoning* 116024, *China*)

Abstract: Two cobalt complexes containing NSP (nitrogen-sulphur-phosphor) chelator prepared from thiosemicarbazone ligands with different terminal functional groups and triphenylphosphine moiety have been synthesized in high yield and characterized. Their photocatalytic activity for hydrogen evolution under visible light irradiation was investigated. The photocatalyst [Co(L2)(L2′)]$(BF_4)_{2.5}\cdot H_2O\cdot 0.5C_2H_5OH$ (**2**) (L2=2-(diphenylphosphino)benzylidene-2-(3, 6-bis(ethylamino)-2, 7-dimethyl-9*H*-xanthen-9-yl)benzothiohydrazide, L2′=2-(diphenylphosphinooxide)benzylidene-2-(3, 6-bis (ethylamino)-2, 7-dimethyl-9*H*-xanthen-9-yl) benzothiohydrazide) containing rhodamine groups exhibited activity in light driven hydrogen evolution with the TON and initial TOF reaching to 2 800 $mol_{H_2}\cdot mol_{cat}^{-1}$ and 930 $mol_{H_2}\cdot mol_{cat}^{-1}\cdot h^{-1}$, respectively, which is much higher than that of complex [Co(L1)(L1′)]$(BF_4)\cdot 0.5H_2O$ (**1**) (L1=2-(diphenylphosphino)benzylidene hydrazinecarbodithionate, L1′=2-(diphenylphosphinooxide)benzylidene hydrazinecarbodithionate) under similar conditions. The higher catalytic activity was attributed to the potential intermolecular π-π stack interactions between the catalyst **2** and photosensitizer fluorescein (**Fl**) benefiting the photoinduced electron transfer between the photosensitizer and the photocatalyst. CCDC: 1523357; **1**, 1523358, **2**.

Keywords: photoinduced electron transfer; cobalt; thiosemicarbazone; light driven H_2 production

收稿日期:2016-12-21。收修改稿日期:2017-04-25。
国家自然科学基金(No.21531001)资助项目。
*通信联系人。E-mail:hecheng@dlut.edu.cn

0 Introduction

The global increase in CO_2 emissions due to uninhibited fossil fuel use has led to explore new renewable and clean energy resources. Photo-induced catalytic splitting of water to non-carbon-contain fuels, i.e. hydrogen, is a promising approach in converting solar energy into storable chemical energy[1-5]. As a redox reaction, water splitting can be divided into two reactions: (i) water oxidation, to yield O_2 and (ii) water reduction, producing H_2. In an artificial photosynthetic (AP) system, the reductive side of water splitting is the light-driven generation of hydrogen from aqueous protons. A variety of photocatalytic systems have been broadly investigated for solar hydrogen production[6-13]. Most of the photocatalytic H_2-production systems involve three important components: a light-absorbing photosensitizer (PS), a water-reducing catalyst (WRC), and a sacrificial reductant. While noble metal co-catalysts such as Pt and Pd were widely used for photocatalytic H_2 evolution, but the scarcity and high cost of precious metals pose serious limitations to wide use. Hence, the development of efficient catalysts for water reduction to H_2 made of inexpensive, earth-abundant elements such as Fe, Co, Ni, and Cu has become a prime focus of research on light-driven hydrogen generation.

In an effort to find stable earth-abundant WRCs, a few recent reviews on catalysts made of earth-abundant elements for water splitting have been published[14-16]. In particular, thiosemicarbazone ligands have been used as versatile molecules, arising from the possibility to act as N, S-donor systems[17-18]. And the number of potential donor atoms can be increased by using carbonylic compounds that contain additional donor groups in suitable positions for chelation. Moreover, they provide a conventional proton immigration path through the thiolate/thioamide resonance tautomer equilibrium[19-20], which have potential future for multi-electron transfer chemistry in H_2 reduction. And these cobalt thiosemicarbazone complexes have gained much interest and might be promising candidates for proton reduction, in the case that the redox potential of the complex was well modified[21-22]. In this article, we introduced a triphenylphosphine moiety as the additional donor to enhance the coordination ability and modify the redox potential of the metal centres (Scheme 1)[23-24]. Recent advances have reported Ni-bis(diphosphine) complexes act as effective reduction catalysts for electrochemical photocatalytical hydrogen production in homogeneous system[25-26]. We expected that the presence of S and P donors would possibly facilitate the formation of reducing species and increase the catalytic efficiency for the H_2 evolution[27]. Herein, we introduced the rhodamine-modified ligands to improve the light absorption efficiency and electron transfer ability between the catalyst **2** and photosensitizer **Fl**. The photocatalytic activity of catalyst **2** was higher than that of **1** under low catalyst concentration. The photo-induced electron transfer pathway mechanisms for the hydrogen evolution in these cobalt-thiosemicarbazone complexes were also proposed.

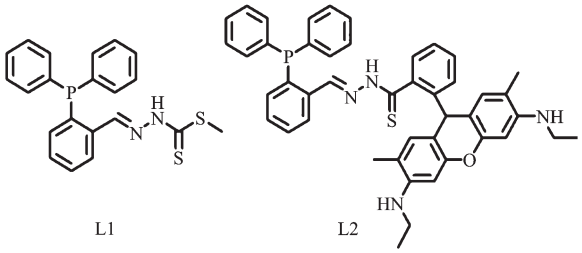

Scheme 1 Structures of thiosemicarbazone ligands L1 and L2

1 Experimental

1.1 Materials and physical measurements

All chemicals were of reagent grade quality obtained from commercial sources and used without further purification. The elemental analyses of C, H and N were performed on a Vario EL Ⅲ elemental analyzer. ^{1}H NMR spectra were measured on a Varian INOVA 400M spectrometer. ESI mass spectra were carried out on a HPLC-Q-Tof MS spectrometer. The fluorescent spectra were measured on a JASCO FP-6500.

Cyclic Voltammogram measurements: Electrochemical measurements of catalysts **1** and **2** were performed in CH_3CN solutions with 0.1 mol·L^{-1}

$TBAPF_6$ working on ZAHNER ENNIUM Electrochemical Workstation with a homemade Ag/AgCl electrode as a reference electrode, a platinum silk with 0.5 mm diameter as a counter electrode, and glassy carbon electrode as a working electrode. The addition of NEt_3HCl (0.1 mol·L^{-1} in CH_3CN) was carried out with syringe.

Fluorescence quenching experiments: A solution (2.0 mL) of **Fl** at 10 μmol·L^{-1} concentration in a EtOH/H_2O solution (1∶1, *V*/*V*, pH=11.6) was prepared in a quartz cuvette fitted with a septum cap, and the solution was degassed under N_2 for 5 min. Aliquots of 20 μL of NEt_3 and the catalysts (2.5 μmol·L^{-1}) were added, and the intensity of the fluorescence was monitored by steady state fluorescence exciting at 460 nm on a Spex Fluoromax-P fluorimeter with a photomultiplier tube detector.

Photocatalytic water splitting experiments: Varying amounts of the catalysts **1** and **2**, **Fl** and NEt_3 in EtOH/H_2O solution (1∶1, *V*/*V*) were added to obtain a total volume of 5.0 mL in a 20 mL flask. The flask was sealed with a septum and degassed by bubbling argon for 15 min. The pH value of this solution was adjusted to a specific pH value by adding HCl or NaOH and measured with a pH meter. After that, the samples were irradiated by a 500 W Xenon lamp with the 400 nm light filter, and the reaction temperature was maintained at 293 K by using a thermostat water bath. The generated photoproduct of H_2 was characterized by GC 7890T instrument analysis using a 5A molecular sieve column (0.6 m×3 mm), thermal conductivity detector, and argon used as carrier gas. The amount of hydrogen generated was determined by the external standard method.

1.2　Synthesis of L1 and L2

The ligand L1 was synthesized by using the reported methods[28]. Anal. Calcd. for $C_{21}H_{19}N_2PS_2$(%): H, 4.85; C, 63.9; N, 7.1; Found(%): H, 5.10; C, 63.3; N, 7.2. ^{1}H NMR ($CDCl_3$, 400 MHz): 10.2 (s, 1H), 8.6 (d, 1H), 8.2 (m, 1H), 7.1~7.5 (m, 13H), 2.6 (s, 3H). API-MS *m*/*z*: 393.07 ([M−H]$^+$).

The ligand L2 was synthesized according to procedures reported previously[29]. Anal. Calcd. for $C_{45}H_{43}N_4SOP$(%): H, 6.03; C, 75.2; N, 7.8; Found(%): H, 6.11; C, 74.9; N, 8.0. ^{1}H NMR ($CDCl_3$, 400 MHz): 9.37 (s, 1H), 8.4 (t, 1H), 8.11 (d, 1H), 8.08 (m, 1H), 7.6~7.7 (m, 4H), 7.4~7.6 (m, 10H), 7.38 (m, 3H), 7.3 (m, 2H), 6.5 (s, 2H), 6.2 (s, 2H), 3.1 (m, 2H), 1.13 (m, 3H); API-MS *m*/*z*: 715.0 ([M−H]$^+$).

1.3　Synthesis of complex 1

The ligand L1 (0.6 mmol, 0.236 g) and $Co(BF_4)_2\cdot 6H_2O$ (0.3 mmol, 0.1 g) was dissolved in 10 mL ethanol. The solution was refluxed for 2 h, and then slowly evaporated at room temperature. The red block crystals were obtained in several days. Yield: ~55%. ESI-MS *m*/*z*: 845.23 for the +1 charge cation. Anal. Calcd. for $CoC_{42}H_{37}N_4OP_2S_4BF_4\cdot 0.5H_2O$(%): H, 3.99; C, 52.6; N, 5.84; Found(%): H, 4.02; C, 52.1; N, 5.89. IR (KBr, cm^{-1}): 3 424 (br), 3 056 (m), 1 630 (s), 1 586 (s), 1 480 (m), 1 460 (m), 1 436 (m), 1 313 (s), 1 127 (m), 1 063 (m), 1 012 (m), 875 (s), 754 (m), 727 (m), 696 (m), 562 (m), 526 (m), 498 (m).

1.4　Synthesis of complex 2

$Co(BF_4)_2\cdot 6H_2O$ (0.05 mmol, 0.017 g) and the ligand L2 (0.05 mmol, 0.035 g) was dissolved in 15 mL of dichloromethane/ethanol (1∶1, *V*/*V*). The solution was stirred at boiling temperature for 2 h to obtain a clear black red solution and allowed to stand at room temperature. The red block crystals suitable for single-crystal X-ray diffraction were obtained. Yield: ~40%. ESI-MS m/z: $(2L2+Co)^{3+}$, 497.16; $(2L2+Co+BF_4)^{2+}$, 789.76. Anal. Calcd. for $CoC_{91}H_{85.5}N_8O_3P_2S_2B_{2.50}F_{10}\cdot H_2O\cdot 0.5C_2H_5OH$(%): H, 5.15; C, 61.7; N, 6.33; Found(%): H, 5.20; C, 61.1; N, 6.37. IR (KBr, cm^{-1}): 3 243 (br), 2 973(s), 1 647 (m), 1 606 (m), 1 560 (m), 1 527 (m), 1 499 (m), 1 446 (s), 1 366 (s), 1 306 (m), 1 243 (m), 1 186 (m), 1 124 (m), 1 083 (m), 944 (s), 882 (s), 748 (s), 693 (m), 611 (m), 522 (s).

1.5　X-ray crystallography

The data were collected on a Bruker Smart APEX Ⅱ X-diffractometer equipped with graphite monochromated Mo *Kα* radiation (*λ*=0.071 073 nm) using the SMART and SAINT[30] programs at 296 K for complexes **1** and **2**. Final unit cell parameters were based on all observed reflections from integration of all frame data. The structures were solved in the

space group by direct method and refined by the full-matrix least-squares using SHELXTL-97 fitting on F^2[31]. For complexes **1** and **2**, all non-hydrogen atoms were refined anisotropically. Except the solvent water molecules, the hydrogen atoms of organic ligands were located geometrically and fixed isotropic thermal parameters. The BF_4^- groups in complex **2** were disordered; therefore, large thermal displacement parameters were found for these atoms and refined with partial occupancy. One of the benzene rings was disordered into two parts with the S. O. F. (sites occupied factor) of each part being fixed as 0.5. One ethylamine moiety and ethyl groups in complex **2** were disordered into two parts with the S.O.F. of each part being fixed as 0.5. The crystal data and details of the structure refinement of complexes **1** and **2** are summarized in Table 1.

CCDC: 1523357; **1**, 1523358, **2**.

Table 1 Crystal data and structure refinements for complexes 1 and 2

Complex	1	2
Formula	$CoC_{42}H_{38}BF_4N_4O_{1.5}P_2S_4$	$CoC_{91}H_{90.5}B_{2.50}F_{10}N_8O_{4.50}P_2S_2$
Formula weight	958.68	1 770.23
Crystal system	Monoclinic	Triclinic
Space group	$P2_1/c$	$P\bar{1}$
a / nm	1.467 5(4)	1.336 92(8)
b / nm	1.541 7(4)	1.917 1(1)
c / nm	1.966 9(5)	2.238 8(1)
α / (°)	90	101.642(4)
β / (°)	91.744(3)	94.854(4)
γ / (°)	90	107.308(4)
V / nm^3	4.448(2)	5.301 1(5)
Z	4	2
D_c / (g·cm^{-3})	1.432	1.109
F(000)	1 968	1 840
Reflection collected	24 141	38 673
Unique reflection (R_{int})	7 846 (0.070 2)	18 616 (0.071 0)
Goodness-of-fit on F^2	1.006	1.022
Final R indices[a,b] [$I>2\sigma(I)$]	R_1=0.053 1, wR_2=0.128 2	R_1=0.086 8, wR_2=0.206 1
Rindices[a,b] (all data)	R_1=0.092 0, wR_2=0.141 8	R_1=0.184 3, wR_2=0.230 9

[a] $R_1=\sum(|F_o|-|F_c|)/\sum|F_o|$; [b] $wR_2=[\sum w(|F_o|-|F_c|)^2/\sum wF_o^2]^{1/2}$.

2 Results and discussion

2.1 Crystal structural description

Single-crystal structure representation for the complexes **1** and **2** are shown in Fig.1. In the crystal of complex **1**, each central cobalt environment can be described as a distorted octahedron, comprising two N, S atoms from thiosemicarbazone groups, one P atoms from the triphenylphosphine group and the O atom originated from oxidized P atom. One of the P atoms in the ligand L1 was oxidized under the synthesis process. The two ligands bind to a cobalt(Ⅲ) in a *mer* configuration as found in the related cobalt thiosemicarbazone complexes[32-33]. The C-S, C-N and N-N bond distances are agreed well with the normal range of single and double bonds, resulting in the extensive electron donation environment over the entire molecular skeleton[34-35]. Similar to the complex **1**, in the crystal of complex **2**, the metal center was octahedrally coordinated by two N, S atoms and a P or O chelator atom that originated from the different ligands L2 and L2′. And the distance between two xanthene rings of rhodamine ligands in adjacent complex was 0.36 nm. The presence of intermolecular strong π-π stacking interactions between the rhodamine groups implied the possibility on the

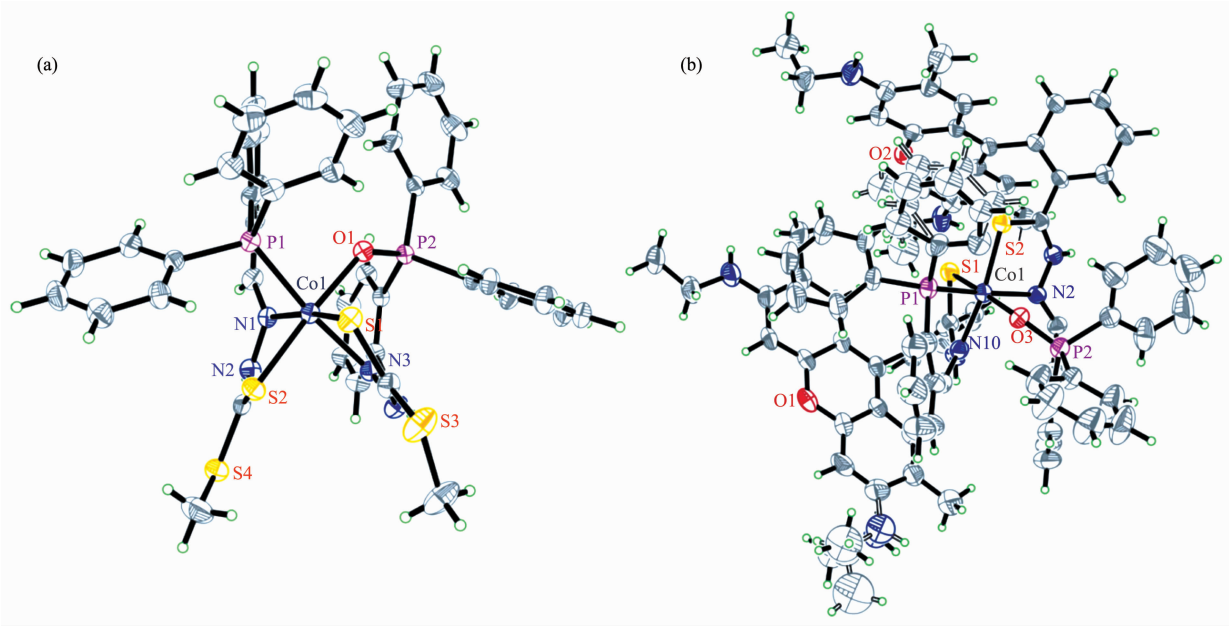

Thermal ellipsoids are drawn at the 30% probability level; Anions and solvent molecules are omitted for clarity; Selected bond distance (nm) in **1**: Co(1)-N(1) 0.197 0(3), Co(1)-O(1) 0.200 6(3), Co(1)-N(2) 0.201 4(3), Co(1)-S(2) 0.222 9(1), Co(1)-P(1) 0.222 2(2), Co(1)-S(1) 0.223 1(1); Selected bond distance (nm) in **2**: Co(1)-N(10) 0.194 7(4), Co(1)-O(3) 0.201 0(4), Co(1)-N(2) 0.203 0(4), Co(1)-S(2) 0.221 3(2), Co(1)-P(1) 0.221 7(2), Co(1)-S(1) 0.223 0(2)

Fig.1 Single-crystal structure representations of **1** (a) and **2** (b) showing the coordination geometry of the metal ion

formation of π-π interaction between complex **2** and the xanthene rings within the photosensitizer **Fl**. As a result, the photogenerated electron would be easily immigrated between the photosensitizer and the photocatalyst during the photoreduction processes, which was beneficial to achieve the high activity in the photocatalytic system[36].

2.2 Cyclic voltammetry of the complexes

The cyclic voltammetry shows that the redox potential of Co(Ⅱ)/Co(Ⅰ) occurs at −1.0 V and −0.87 V for **1** and **2**, respectively. And the complex **2** exhibits one inreversible Co(Ⅲ)/Co(Ⅱ) redox process at −0.6 V. To investigate the role of the Co complex as a WRC catalyst, cyclic voltammetry was performed in the presence of increasing amounts of NEt_3HCl. Addition of NEt_3H^+ with increasing amounts triggers the appearance of a new irreversible cathodic wave near the Co(Ⅱ)/Co(Ⅰ) response[37-38]. Increasing the concentration

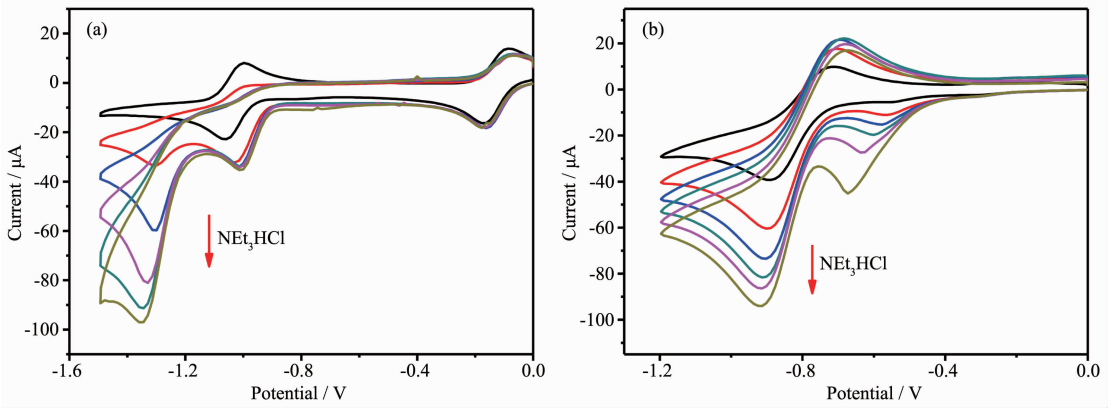

Scan rate: 100 mV·s^{-1}

Fig.2 Cyclic Voltammogram of **1** (a) and **2** (b) (1 mmol·L^{-1}) in CH_3CN with 0.1 mol·L^{-1} $TBAPF_6$ upon addition of NEt_3HCl with different concentrations

of NEt_3H^+ raises the height of the new wave and shifts it to more negative potentials, indicating that complexes **1** and **2** are able to reduce the proton with a catalysis process.This observation indicates direct protonation of the reduced Co(I) center and also shows that the protonation process is fast in the overall catalytic rate.

2.3 Complexes 1 and 2 as efficient quencher for the photosensitizer Fl

Complexes **1** and **2** also serves as an efficient quencher for the photosensitizer **Fl**. To verify this hypothesis further, the Stern-Volmer quenching constant K_q in this system was calculated as 1.9×10^4 $L\cdot mol^{-1}$ upon the addition of **1** into **Fl** solution in EtOH/H_2O (1:1, *V*/*V*). The quenching behavior can be considered as a photoinduced electron transfer process from excited state of **Fl*** to **1**, providing possibilities for **Fl** to activate complex **1** producing H_2 in solution. Although the K_q for the catalyst **1** was higher than that reported for NEt_3 (0.44 $L\cdot mol^{-1}$), the concentration of NEt_3 (1.08 $mol\cdot L^{-1}$, 15%) in the actual photocatalytic reactions is much higher than the catalyst **1** (10 $\mu mol\cdot L^{-1}$). A photoinduced electron transfer from the NEt_3 to the excited state of **Fl** (reduction quenching) dominated the homogeneous photolysis of the reaction mixture instead of direct quenching by **1**. As the Stern-Volmer quenching constant of **2** (9.85×10^4 $L\cdot mol^{-1}$) is higher than that of complex **1** (Fig.3). It indicates that the modified rhodamine group was in favor of the electronic transport between the catalyst **2** and photosensitizer **Fl**. When the concentration of NEt_3 was fixed at 0.5 $mol\cdot L^{-1}$ (7%, *V*/*V*) and catalyst **2** was fixed at 10 $\mu mol\cdot L^{-1}$ under the photocatalytic condition, the direct luminescence quenching of **Fl** by the catalyst **2** should be largely dominated by the oxidative quenching. The initial photochemical step was the formation of Fl^+ caused by **2**[39-40]. Because both the photosensitizer Fl and the rhodamine-based catalyst contain highly conjugated xanthene moieties, **Fl** molecules might have strong π-π stacking interact with the catalyst **2**, which is beneficial to transfer electrons from the photoexcited Fl^* to **2**[41]. This process led to a more efficient separation of the photogenerated electrons, thus suppressing the combination of electrons that would result in undesired radiative transition. Therefore, the photo-induced electron transfer pathway obtained by the catalyst **2** could potentially be benefit for the construction of efficient photocatalytic systems.

2.4 Complex 1 as a WRC

Proton reduction catalytic activity of **1** was evaluated by coupling it with **Fl** as a photosensitizer (PS) upon irradiation with visible light (λ>400 nm) in an EtOH/H_2O (1:1, *V*/*V*) solvent mixture containing NEt_3 at room temperature[42-44]. The optimum pH value of the reaction mixture was maintained at 11.5, decreasing or increasing pH values resulted in both a lower initial rate and shorter system lifetime for hydrogen evolution (Fig.4a). The efficiency of the

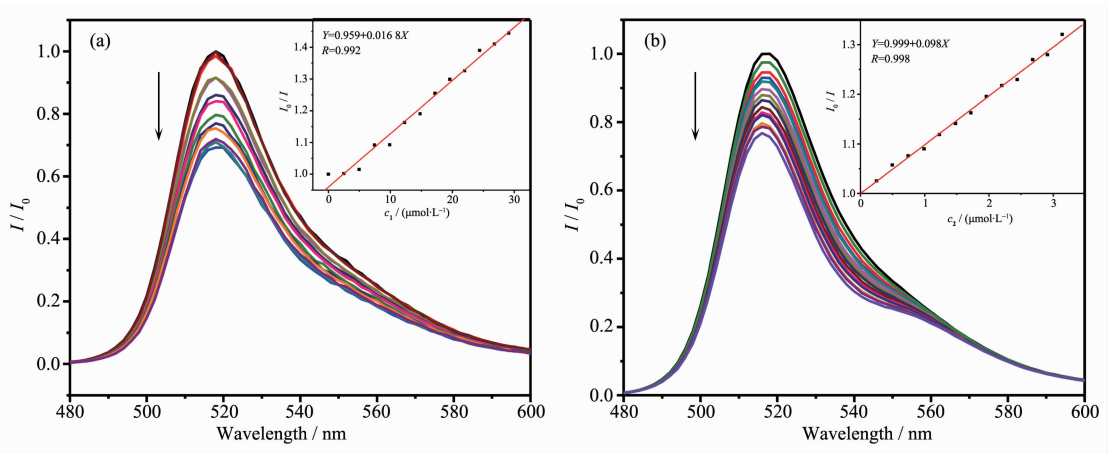

Inset: Stern-Volmer plot for the photoluminescence quenching of **Fl** by catalysts **1** and **2**

Fig.3 Family of the emission spectra of fluorescein solution (10 $\mu mol\cdot L^{-1}$) in EtOH/H_2O (1:1, *V*/*V*) solution upon addition of catalyst **1** (a) and **2** (b) with various concentration

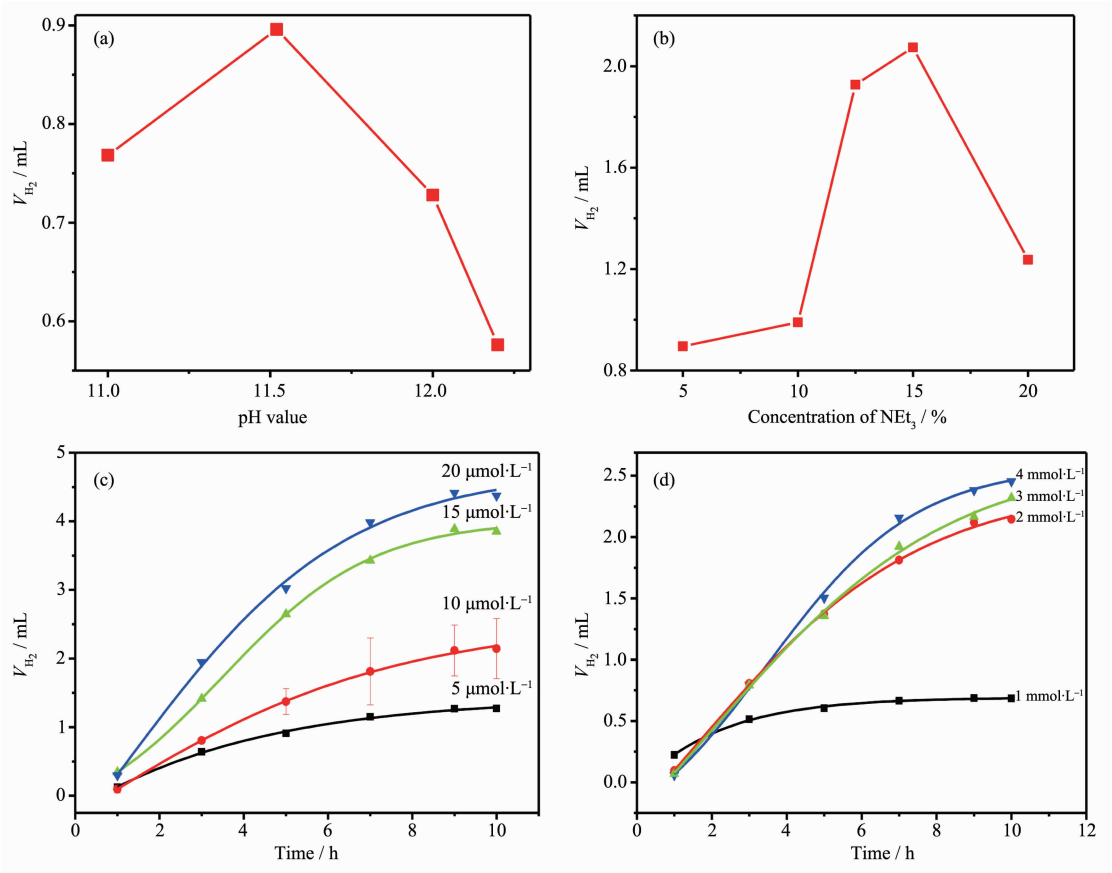

c_1=10.0 μmol·L^{-1}, c_{Fl}=2.0 mmol·L^{-1} for (a) and (b); c_1=5.0, 10.0, 15.0, 20.0 μmol·L^{-1}, c_{Fl}=2.0 mmol·L^{-1} for (c); c_1=10.0 μmol·L^{-1}, c_{Fl}=1.0, 2.0, 3.0, 4.0 mmol·L^{-1} for (d)

Fig.4　Initial rates of H_2 production in systems containing **1**, **Fl** and 15% (*V*/*V*) of NEt_3 with different pH values (a) and containing **1**, **Fl** at pH 11.5 with different concentrations of NEt_3 (b); Photocatalytic hydrogen evolution of systems containing **Fl**, 15% (*V*/*V*) NEt_3 with different concentrations of **1** (c) and containing **1**, 15% (*V*/*V*) NEt_3 with different concentrations of **Fl** (d)

visible light induced hydrogen evolution depends on the concentration of sacrificial reagent NEt_3. The optimal concentration is 15%, with a decrease of activity at lower or higher concentration. Furthermore, the addition of two of the three components of the homogeneous systems could not give any further H_2 evolution which indicated that both the **1** and **Fl** were decomposed during the photolysis.

In the system with **Fl** and NEt_3 at fixed concentrations, the initial rate of H_2 generation exhibits a first-order dependence on catalyst **1**. At 10.0 μmol·L^{-1} catalysts **1** and 2 mmol·L^{-1} **Fl**, this system exhibits a TON of 2 267 mol_{H_2}·mol_{cat}^{-1} after 10 hours and an initial TOF of 220 mol_{H_2}·mol_{cat}^{-1}·h^{-1}. At higher catalyst concentrations, even though a larger amount of H_2 is evolved, the TON does not scale linearly with catalyst concentration due to the limited lifetime of the system. To determine the limit of this system, an additional experiment was carried out at different **Fl** concentrations shown in Fig.4d. At higher **Fl** concentration as 4 mmol·L^{-1}, there is no continuous increased H_2 generation detected in 10 h. The TOF reaches a maximum at 2.0 mmol·L^{-1} **Fl**, which indicates that the system is limited by the concentration of the catalyst. The system has a longer life time at higher **Fl**, thus suggesting that **Fl** decomposes during photolysis. This phenomenon also demonstrates that the reductive quenching path way dominates in the system of catalyst **1**.

2.5　Complex 2 as a WRC

Through investigating the influence of different pH values and concentration of NEt_3, we found the

highest efficiency of H_2 production could be achieved at pH 11.6 and NEt_3 7%. For initial experiments, the **Fl** concentration in the reaction vials was kept at 2 mmol·L^{-1}, while a 5 μmol·L^{-1} catalyst concentration was chosen. The initial TOF calculated was 346.5 mol_{H_2}·mol_{cat}^{-1}·h^{-1} in 5 h with the TON of about 1 732 mol_{H_2}·mol_{cat}^{-1}. To further probe the photocatalytic process, concentrations of both the **Fl** and the catalyst **2** were varied. Details of the effect of reactant concentration on H_2 evolution are depicted in Fig.5. In terms of catalyst turnovers, it was observed that the photocatalytic system performs better at high **Fl** concentration and low catalyst concentration. These results pointed toward high degradation degree of the catalyst **2**, which was more notable at higher concentrations. As shown in Table 2, in the same reaction condition, catalyst **2** has a higher TON and TOF than catalyst **1** in the concentration of 5 μmol·L^{-1} for catalyst. However, in the higher catalyst concentration of 20 μmol·L^{-1}, the catalyst **1** showed the better photocatalytic activity than catalyst **2**. It was attribute to the self-stacking interaction of rhodamine group in high concentration which reduced the electronic transfer ability between the catalyst **2** and **Fl**. And in the same catalyst concentration, catalyst **2** exhibited higher TON and TOF than catalyst **1** in different **Fl** concentration in 5 h. These results demonstrated that the fast electronic transfer in catalyst **2** was benifit for the photocatalytic system in low catalyst concentration. When the concentration of the catalyst was lowered from 5 μmol·L^{-1} to 1 μmol·L^{-1}, keeping the **Fl** at the optimal concentration, the hydrogen evolution continued within 3 hours. Although the quantity of hydrogen production decrease, it led to a large

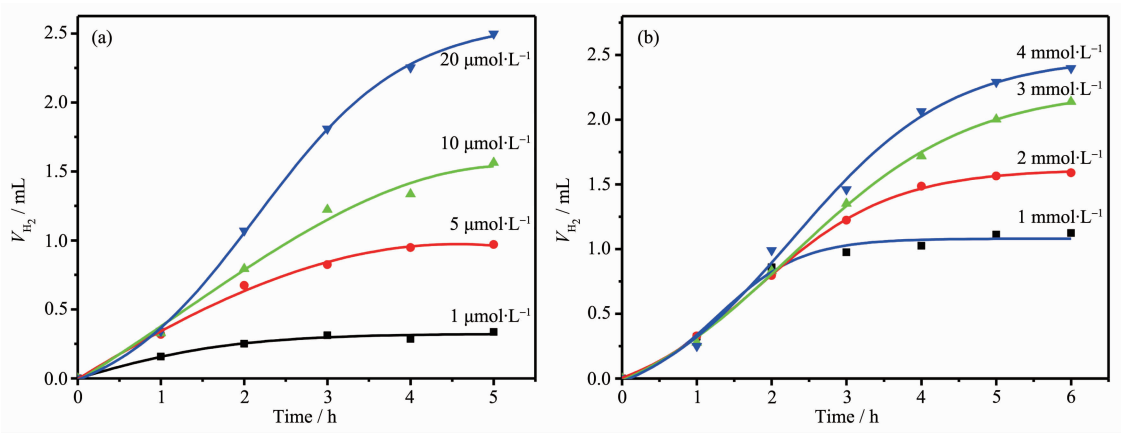

Concentration of NEt_3: 7% (*V*/*V*); c_{Fl}=2.0 mmol·L^{-1}, c_2=1.0, 5.0, 10.0, 20.0 μmol·L^{-1} for (a); c_2=10.0 μmol·L^{-1}, c_{Fl}=1.0, 2.0, 3.0, 4.0 mmol·L^{-1} for (b)

Fig.5 Photocatalytic hydrogen evolution of systems containing **Fl**, NEt_3 with different concentrations of **2** (a) and containing **2**, NEt_3 with different concentrations of **Fl** (b)

Table 2 Data of hydrogen production test in 5 h for complexes 1 and 2

Entry*	TON / (mol_{H_2}·mol_{cat}^{-1})		TOF / ((mol_{H_2}·mol_{cat}^{-1}·h^{-1})	
	1	**2**	**1**	**2**
1	1 620.5	1 732.5	324.1	346.5
2	1 224.6	1 396.7	244.9	279.3
3	1 348.6	1 115.2	269.7	223.0
4	539.0	1 003.1	107.8	200.6
5	1 224.6	1 396.7	244.9	279.3
6	1 227.6	1 911.0	245.5	382.2
7	1 342.9	2 140.9	268.5	428.1

* Entry **1**~**3**: c_{Fl}=2 mmol·L^{-1}, c_{cat}=5, 10, 20 μmol·L^{-1}, respectively; Entry **4**~**7**: c_{cat}=10 μmol·L^{-1}, c_{Fl}=1, 2, 3, 4 mmol·L^{-1}, respectively.

increase in turnovers yielding up to 2 800 $mol_{H_2} \cdot mol_{cat}^{-1}$ and the highest TOF 930 $mol_{H_2} \cdot mol_{cat}^{-1} \cdot h^{-1}$.

The light induced H_2 evolution varied on the concentration of **Fl**, and the increasing of **Fl** amount caused the increasing of TON. These results suggest both the **2** and **Fl** were decomposed during the photolysis, but the decompose rate of **Fl** was much higher than that of the catalyst **2**. The photocatalytic activity of catalyst **2** was decreased after 5 h, while catalyst **1** showed better activity in 10 h. The life time of the hydrogen evolution system was shorten, which could be due to the cooperation effect between rhodamine groups and **Fl**. This fast energy transfer process resulted the quick decompose of **Fl** and catalyst **2**. Relative to catalyst **1**, catalyst **2** has a higher hydrogen production rate in the beginning of the reaction process which also demonstrated the fast electron transfer in rhodamine-modified systems. A tentative mechanism proposed for the high activity of catalyst **2** for the production of H_2 has been deduced. Photogenerated electrons in **Fl** firstly transfer to the rhodamine groups in **2** under illumination with visible light through the possible intermolecular π-π interactions, and then the ligands transfer electrons to the Co center, where H_2 evolution reactions occur. At last, the electron donor NEt_3 restore the excited $\mathbf{Fl}^+$ to the ground state to complete the catalytic cycle.

3　Conclusions

In summary, we reported a simple but effective method to gain cobalt-thiosemicarbazone complexes **1** and **2** as the efficient water reductive catalyst. Structures of these complexes were determined by single crystal X-ray analysis. Electrochemical analysis demonstrated their WRC activity in presence of a proton source of NEt_3HCl. The water reduction properties of the catalyst were evaluated using **Fl** as PS with NEt_3 as the sacrificial donor. Introducing the rhodamine group which could cooperate with the photosensitizer makes the catalyst **2** more efficient with the TON and initial TOF reaching to 2 800 $mol_{H_2} \cdot mol_{cat}^{-1}$ and 930 $mol_{H_2} \cdot mol_{cat}^{-1} \cdot h^{-1}$. The higher photocatalytic activity in lower catalyst concentration and short time indicates the fast electron transfer ability between the catalyst **2** and photosensitizer **Fl**. The photocatalytic process is dominated by the oxidative quenching with the formation of $\mathbf{Fl}^+$ caused by **2** which is benefit for the hydrogen evolution. All these work declare the bright future of the thiosemicarbazone complex in hydrogen evolution.

References:

[1] Cook T R, Dogutan D K, Reece S Y, et al. *Chem. Rev.*, **2010**,**110**:6474-6502

[2] Bard A J, Fox M A. *Acc. Chem. Res.*, **1995**,**28**:141-145

[3] Chen X, Liu L, Yu P Y, et al. *Science*, **2011**,**331**:746-750

[4] Wang F, Wang W G, Wang X J, et al. *Angew. Chem., Int. Ed.*, **2011**,**50**:3193-3197

[5] Yuhas A D, Smeigh A L, Douvalis A P, et al. *J. Am. Chem. Soc.*, **2012**,**134**:10353-10356

[6] Kluwer A M, Kapre R, Hartl F, et al. *PNAS*, **2009**,**106**:10460-10465

[7] Zhang P, Wang M, Li C, et al. *Chem. Commun.*, **2010**,**46**:8806-8808

[8] McNamara W R, Han Z, Alperin P J, et al. *J. Am. Chem. Soc.*, **2011**,**133**:15368-15371

[9] McCormick T M, Calitree B D, Orchard A, et al. *J. Am. Chem. Soc.*, **2010**,**132**:15480-15483

[10]McLaughlin M P, McCormick T M, Eisenberg R, et al. *Chem. Commun.*, **2011**,**47**:7989-7991

[11]Han Z, McNamara W R, Eum M S, et al. *Angew. Chem. Int. Ed.*, **2012**,**51**:1667-1670

[12]Zhang W, Hong J, Zheng J, et al. *J. Am. Chem. Soc.*, **2011**,**133**:20680-20683

[13]WEN Fu-Yu(温福宇), YANG Jin-Hui(杨金辉), ZONG Xu(宗旭), et al. *Prog. Chem.*(化学进展), **2009**,**21**(11):2285-2302

[14]Artero V, Chavarot-Kerlidou M, Fontecave M. *Angew Chem, Int Ed.*, **2011**,**50**:7238-7266

[15]Lin Y, Yuan G, Sheehan S, et al. *Energy Environ. Sci.*, **2011**,**4**:4862-4869

[16]Lobana T S, Sharma R, Bawa G, et al. *Coord. Chem. Rev.*, **2009**,**253**:977-1055

[17]Beraldo H, Gambino D. *Mini Rev. Med. Chem.*, **2004**,**4**:31-39

[18]Milunovic M N M, Enyedy E A, Nagy N V, et al. *Inorg. Chem.*, **2012**,**51**:9309-9321

[19]Peng H, Liu G F, Liu L, et al. *Tetrahedron*, **2005**,**61**:5926-5932

[20]AliM A, Bernhardt P V, Brax M A H, et al. *Inorg. Chem*., **2013**,**52**:1650-1657

[21]Chang T M, Tomat E. *Dalton Trans*., **2013**,**42**:7846-7849

[22]Credico A, de Biani F F, Gonsalvi L, et al. *Chem. Eur. J*., **2009**,**15**:11985-11998

[23]Zhang L Y, Xu L J, Zhang X, et al. *Inorg. Chem*., **2013**,**52**: 5167-5175

[24]Han Z J, Shen L X, Brennessel W W, et al. *J. Am. Chem. Soc*., **2013**,**135**:14659-14669

[25]Goff A L, Artero V, Jousselme B, et al. *Science*, **2009**,**326**: 1384-1387

[26]Kilgore U J, Roberts J A S, Pool D H, et al. *J. Am. Chem. Soc*., **2011**,**133**:5861-5872

[27]Du P, Eisenberg R. *Energy Environ. Sci*., **2012**,**5**:6012-6021

[28]Jing X, Wu P, Liu X, et al. *New J. Chem*., **2015**,**39**:1051-1059

[29]Huang W, Song C, He C, et al. *Inorg. Chem*., **2009**,**48**:5061 -5072

[30]*SMART*, *SAINT* and *XPREP*, Bruker Analytical Instruments Inc., Madison, WI, **1995**.

[31]Sheldrick G M. *SHELXS*-97, *Program for X-ray Crystal Structure Solution and Refinement*, University of Göttingen, Germany, **1997**.

[32]Duan C Y, Liu Z H, You X Z, et al. *Chem. Commun*., **1997**: 381-382

[33]Li M X, Chen C L, Zhang D, et al. *Eur. J. Med. Chem*., **2010**,**45**:3169-3177

[34]Katti K V, Singh P R, Barnes C L. *J. Chem. Soc., Dalton Trans*., **1993**:2153-2159

[35]ZhaoY G, Guo D, Liu Y, et al. *Chem. Commun*., **2008**:5725-5727

[36]Stewart M P, Ho M H, Wiese S, et al. *J. Am. Chem. Soc*., **2013**,**135**:6033-6046

[37]Razavet M, Artero V, Fontecave M. *Inorg. Chem*., **2005**,**44**: 4786-4795

[38]Kasunadasa H I, Chang C J, Long J R. *Nature*, **2010**,**464**: 1329-1333

[39]Zhang P, Wang M, Dong J, et al. *J. Phys. Chem. C*, **2010**, **114**:15868-15874

[40]Li L, Duan L L, Wen F Y, et al. *Chem. Commun*., **2012**,**48**: 988-990

[41]Dong X Y, Zhang M, Pei R B, et al. *Angew. Chem. Int. Ed*., **2016**,**55**:2073-2077

[42]Lazarides T, McCormick T, Du P W, et al. *J. Am. Chem. Soc*., **2009**,**131**:9192-9194

[43]HAN A-Li(韩阿丽), DU Ping-Wu(杜平武). *Chinese J. Inorg. Chem.*(无机化学学报), **2013**,**29**(8):1703-1709

[44]Zhang P, Wang M, Na Y, et al. *Dalton Trans*., **2010**,**39**:1204 -1206